# Dynamics of polyacetylene chains

Francisco Guinea*
*Institute for Theoretical Physics, University of California, Santa Barbara, California 93106*
(Received 13 February 1984)

The dynamics of polyacetylene chains have been studied using the Su-Schrieffer-Heeger Hamiltonian and within the adiabatic approximation. We investigate the nature of the various nonlinear excitations of the system, as well as their interactions. It is shown that both solitons and breathers are highly stable and regain their shape after undergoing collisions with remarkable accuracy. A detailed analysis of soliton-antisoliton scattering is given, as well as its effect on the electronic properties of the system.

## I. INTRODUCTION

The standard theoretical model for the understanding of polyacetylene is the Su-Schrieffer-Heeger (SSH) Hamiltonian[1,2] which focuses on the coupling between the $\pi$ electrons and the ionic motions along the one-dimensional polymer chain. It is well known that this model exhibits a rich variety of nonlinear phenomena and topological excitations. In particular, molecular-dynamics studies of optical absorption[3,4] provide a simple interpretation of experimental data in terms of soliton-antisoliton production.[5]

The purpose of this paper is to carry these studies further and analyze systematically the properties of the nonlinear excitations of $(CH)_n$ within the adiabatic approximation. In Sec. II I present the method of calculation and discuss its limitations and advantages. Then, the method is applied to analyze the detailed structure of static and moving solitons.

In the following sections the main results of this paper, the dynamics of solitons and soliton-antisoliton and soliton-breather collisions, will be presented, as well as their effects on the electronic properties of the system. Finally, a discussion of the most relevant features of this analysis will conclude the paper.

## II. METHOD OF CALCULATION

As mentioned above, we will use the SSH Hamiltonian to describe polyacetylene,

$$\begin{aligned} H_e &= t\sum_{i,\sigma} c^{\dagger}_{i+1,\sigma}c_{i,\sigma} + \text{H.c.} \ , \\ H_{\text{ph}} &= \sum_i \frac{P_i^2}{2M} + \sum_i \frac{K}{2}(x_{i+1}-x_i)^2 \ , \\ H_{e\text{-ph}} &= \alpha\sum_{i,\sigma} c^{\dagger}_{i+1,\sigma}c_{i,\sigma}(x_{i+1}-x_i) + \text{H.c.} \ , \end{aligned} \tag{1}$$

with parameters[2] $t=2.5$ eV, $K=21$ eV Å$^{-2}$, and $\alpha=4.1$ eV Å$^{-1}$, which give a dimerization parameter of 0.04 Å and a soliton width of about $14a$, where $a$ is the lattice constant of the undimerized chain.

In order to follow the time evolution of the system, we will make use of the adiabatic approximation, and assume that the ions obey Newton's equations of motion, with well-defined classical trajectories. For each set of atomic coordinates, the electrons rearrange themselves to minimize their energy. Owing to the large difference between the ionic and the electronic mass, $M_i = 24\,000 m_e$, this is a very reasonable approximation, as further supported by Monte Carlo simulations and renormalization studies of the full quantum Hamiltonian.[8] It is to be noted that quantum effects associated with the small soliton mass cannot be ruled out, although quantum corrections to its value seem to be small.[7]

For each set of ionic coordinates $\{x_j\}$, we have to solve the following equations:

$$\begin{aligned} M_i\ddot{x}_i &= K(2x_i - x_{i+1} - x_{i-1}) + F_e^i \ , \\ F_e^i &= -\frac{\partial}{\partial x_i}\langle \psi_e \mid H(\{x_j\}) \mid \psi_e \rangle \ , \end{aligned} \tag{2}$$

where $\psi_e$ is the wave function of the ground state of $H(\{x_j\})$ with the required number of electrons. As it is an eigenstate of $H$, we can use the Feynman-Hellmann theorem to calculate $F_e$:

$$F_e^i = 2\alpha\sum_{\sigma}\langle \psi_e \mid c^{\dagger}_{i+1,\sigma}c_{i,\sigma} - c^{\dagger}_{i,\sigma}c_{i-1,\sigma} \mid \psi_e \rangle \tag{3}$$

and the quantity on the right-hand side of (3) can be expressed in terms of Green's functions,

$$\langle \psi_e \mid c^{\dagger}_{i+1,\sigma}c_{i,\sigma} \mid \psi_e \rangle = -\frac{1}{\pi}\int_{-\infty}^{\epsilon_F} \text{Im}[G_{i+1,\sigma;i,\sigma}(\omega)]d\omega \ , \tag{4}$$

where $\epsilon_F$ is the energy of the uppermost occupied electronic level in the system. A variety of methods exist to calculate Green's functions in one-dimensional systems,[8,9] which avoid the need to diagonalize large matrices; the ones used here are described in detail in the Appendix. It should be noted that in order to perform the integral in (4), a small imaginary part, $\sim 0.01$ eV, has been included in the energies, in order to round off the peaks in the Green's functions. Note that this procedure is different from the one followed in Refs. 3 and 4. The main differences are the direct calculation of the forces and the avoidance of manipulations of large matrices. This allows us to study larger chains as considered previously.

To minimize end effects, the calculations have been performed for chains whose ends are attached to an infin-

 

ite number of atoms clamped in rigid positions, or for closed rings of atoms. Both geometries have the extra advantage of preventing a global shrinking of the polymer backbone which leads to a renormalization of the parameters to be used in the Hamiltonian, but with no physical consequences. The equations of motion (2) are integrated using standard numerical procedures. In cases where inversion symmetry is preserved, only half of the equations are actually solved.

## III. PROPERIES OF STATIC AND MOVING SOLUTIONS

Once the forces on the atoms are calculated, it is simple to analyze equilibrium properties of the polymer chains by setting all forces [Eq. (2)] equal to zero and solving the resulting set of nonlinear equations for the atomic displacements. We have applied this method to study solitons at rest, obtained by matching a linear chain of atoms to infinite chains dimerized in opposite phases at both ends. We let an odd number of atoms readjust freely so that the system is symmetric around the central atom, and there is only a need to solve for half of the equations.

The results for the order parameter, $u_i=(-1)^i x_i$, where $x_i$ is the displacement from the equilibrium nondimerized position of atom $i$, and the change in bond length, $y_i=u_i+u_{i+1}$, are depicted in Fig. 1. The chain shrinks near the soliton, inducing a linear shift in the atoms far away from it, which is shown in the large oscillations in the order parameter $u_i$, although the total shrinking is about 0.1 Å for the entire soliton. The bond lengths, which are the coordinates with real physical significance, are perfectly dimerized over most of the length of the chain. The details of this spontaneously induced dimerization can be used as a check on the accuracy of the numerical calculations; we estimate that the errors in the coordinates of the atoms are less than 0.002 Å. Near the center of the soliton, the bond lengths follow the hyperbolic tangent shape predicted by the continuum approximation very closely.[10,11] It should be noted that this global shrinking of the chain near a soliton has been found in independent studies,[4] and can have some relevance as it influences the interactions between neighboring chains.[12,13] A simple explanation can be found within the continuum approximation, as periodic metallic chains tend to be slightly shorter than dimerized chains with the same number of atoms; the soliton can be looked upon as a small portion of "metallic" polyacetylene, embedded in a semiconducting background.

It is interesting also to note that there are two slightly different sets of equilibrium coordinates for the soliton, depending on whether $4n+1$ or $4n+3$ atoms are allowed to relax, but otherwise independent of $n$. We think this is a feature associated with end effects which should persist in very long chains; details are shown in Fig. 2.

Solitons in motion have been studied by integrating Eq. (2) for a ring with an odd number of atoms. The dimerization cannot be perfect, and one soliton is generated spontaneously; in this way, the need to deal with a soliton and an antisoliton at the same time is avoided. On the other hand, charge-conjugation symmetry is broken, and the valence and conduction bands are not equivalent. To minimize this effect, very large rings have been considered. Finally, since a constant displacement for the atoms in the ring has no physical significance, only the bond lengths will be studied.

Because of the odd number of atoms, the order parameter defined as $y_i=u_i+u_{i+1}$ seems to change sign each time we go around the ring, as if there was an artificial discontinuity at some point, which we chose to be the atom labeled 1. It is easy to see that all physical properties change smoothly over the ring.

The initial conditions are always of the form

$$u_i=u_0\tanh\left[\frac{x-vt}{\xi(v)}\right], \tag{5}$$

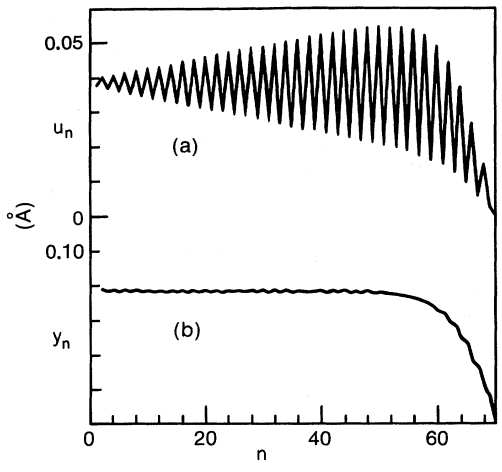


FIG. 1. Equilibrium shape of the soliton. The positions of 139 atoms held between two perfectly dimerized chains have been calculated so the net force acting on each of them is zero. Only half of the chain is shown. (a) Order parameter $u_i=(-1)^i x_i$ ($x_i$, position of atom $i$); (b) bond lengths $y_i=u_{i+1}+u_i$.

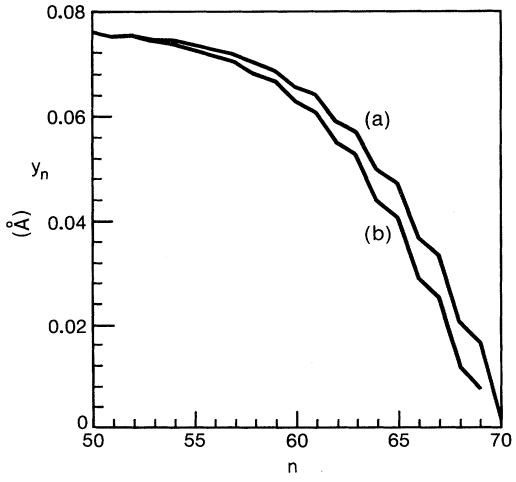


FIG. 2. Different possible shapes of the soliton. Bond lengths are shown, as defined in Fig. 1 (see text for details). (a) 139 atoms; (b) 137 atoms.

where $u_0$ is the equilibrium order parameter for very long chains, and $\xi(v)$, the length of the soliton, is allowed to vary, to obtain the most stable shape as the soliton evolves in time. As a check in the calculation, we estimate that the total energy is conserved within less than $10^{-3}$ eV per atom of the ring. As in other nonlinear field theories,[14] there is a maximum velocity above which the soliton cannot propagate,[4] which, for the choice of parameters used, is $v=4.8\times10^6$ cm/s or $2.6v_s$, where $v_s$ is the velocity of sound of metallic polyacetylene.

Figure 3 shows the motion of solitons for two different initial velocities and shapes. It can be appreciated that the propagation is almost uniform, which is consistent with the fact that discrete lattice effects are very small, in particular the energy for the soliton to hop from site to site. There is a small, velocity-dependent shrinking, similar in some ways to the one found in more conventional nonlinear topological solitons.[14] It should be noted, however, that the solition width does not decrease below 10 Å, in good agreement with simple estimates of this quantity.

In Fig. 4 results obtained by using Eq. (5) as an initial condition are displayed, but with velocities higher than the maximum velocity of the soliton reported earlier. It can be seen that the soliton slows down rapidly, until it moves at roughly the maximum velocity. In addition, a new structure develops, which takes most of the extra energy initially in the soliton; its amplitude grows as the velocity of the soliton is increased. It is in many ways similar to the "breather" solutions found in other nonlinear theories,[4,14] and remains highly stable as the simulation evolves. It is mainly built up of phonons of wavelength $\sim 15a$, i.e., very similar to the soliton width, which are prevented from spreading out by their nonlinear interactions; as will be discussed later, large-amplitude breathers change smoothly into bound soliton-antisoliton pairs.

All the results presented here are obtained by keeping the Fermi energy fixed at the center of the gap, that is, for neutral chains. Hence, no other nonlinear excitations are

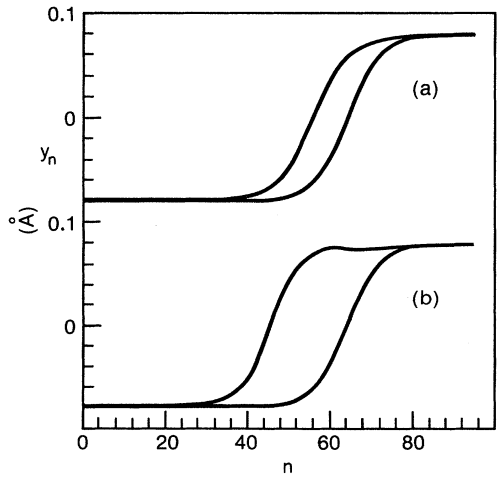


FIG. 3. Soliton moving around a ring of 95 atoms. Bond lengths are shown. For each initial condition the positions of the atoms at $c=7.2\times10^{-14}$ s are also shown. (a) Initial velocity $V_i=1.6\times10^6$ cm/s; (b) $V_i=4\times10^6$ cm/s.

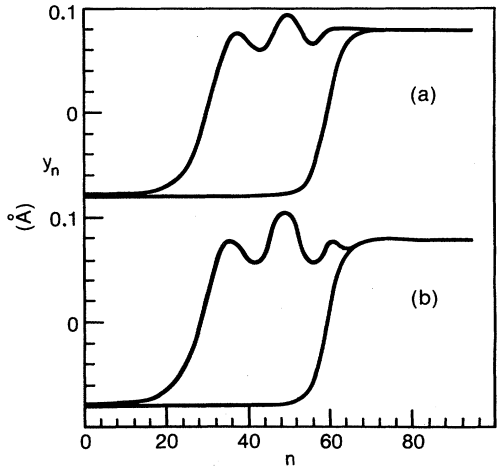


FIG. 4. As in Fig. 3: (a) $V_i=5.6\times10^6$ cm/s; (b) $V_i=8\times10^6$ cm/s.

expected, as polarons[15] explicitly require the presence of extra electrons or holes in the chain. This point will be discussed further in connection with the nature of soliton-antisoliton collisions.

## IV. SOLITON-BREATHER AND SOLITON-ANTISOLITON COLLISIONS

We will now further examine the stability of the nonlinear modes described earlier by studying the collisions between them. While solitons are obviously stable because of topological reasons, nothing prevents a breather or a soliton-antisoliton pair from decaying. In some simple one-dimensional (1D) systems, such as the classical sine-Gordon equation,[14] extra conservation laws impose their stability, and in others, such as the $\varphi^4$ field,[15] numerical simulations show that they are also remarkably stable. It will be shown that this is the case in polyacetylene.

In order to study soliton-breather collisions we generate a breather and a soliton in a ring by using the method described earlier, namely by setting up the initial conditions so that the soliton velocity is higher than its maximum allowed velocity. The breather propagates at slower speed and the soliton moves around the ring and eventually collides with it. Diagrams of the process at different times are shown in Fig. 5. It can be seen that the breather slowly broadens, although most of the energy remains concentrated in a small region of space. During the collision it is difficult to appreciate the shape of the breather; shortly afterwards, however, it regains its form and evolves independently of the soliton.

Soliton-antisoliton collisions will be first studied in the frame of reference at which the "center of mass" of the pair is at rest. Furthermore, we will now study neutral solitons. In this way the ionic motions are symmetric around that point, and only the movements of half of the atoms in the ring have to be considered. Figures 6 and 7 show how the collision proceeds for two different initial velocities of the solitons. In the first case, the pair evolves into a bound state, in which the solitons never separate beyond a certain distance. Most of the time, however,

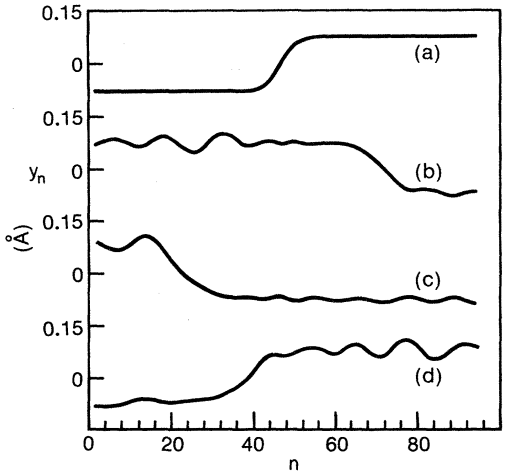


FIG. 5. Collision between a soliton and a breather on a ring with 95 atoms: (a) Initial condition ($v_{sol}=5.6\times10^6$ cm/s), (b) after $9\times10^{-6}$ s, (c) after $17.2\times10^{-6}$ s, and (d) after $27\times10^{-6}$ s.

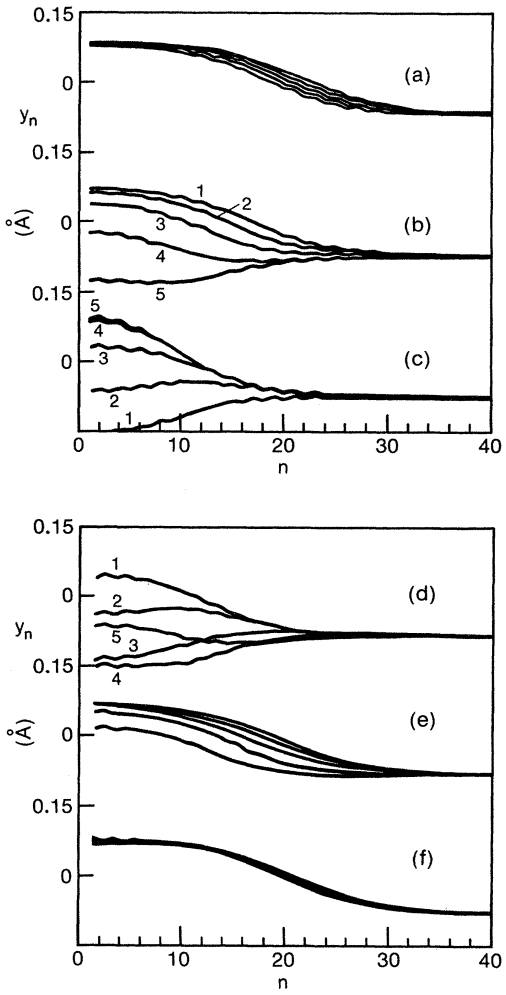


FIG. 6. Collision between solitons on a ring of 184 atoms. The positions of the atoms are symmetrical around the center of mass of the system, and only the time evolutions of half of them have to be computed. The figure shows the 40 atoms closest to the center of mass, the initial velocity of the solitons where $1.6\times10^6$ cm/s. Each diagram is separated from the next by an interval of $7\times10^{-15}$ s. Note that in (f) the solitons come to rest. Not shown is the next collision, which repeats the previous sequence.

they can be distinguished, and the actual collisions take a small fraction of the total "period" of the motion. It is interesting to note that the order parameter behaves in a way very similar to what has been found in simulations of the $\varphi^4$ classical field.[15] When the solitons make contact the order parameter goes to zero and then overshoots, as if the solitons were going to pass through each other, although it is a higher-energy state. The solitons are then repelled, move away, stop, and collide again; after two bounces they regain their shape and separate. This process seems to be independent of the initial velocity of the soliton (also see Fig. 7) and indicates that the kinetic energy of the solitons is transferred into other kinds of collective motions, and only the second time the solitons collide is it again available to let them move away. This behavior has also been reported in the $\varphi^4$ field, although then there is evidence for one, three, etc., bounce collisions, which we have not found in this case. It should be noted that each entire collision takes a time of the order of the inverse optical-phonon frequency ($\omega_0=2\sqrt{K/M}=2.5\times10^{14}$ $s^{-1}$).

Above a certain threshold, the solitons separate to infinity, with velocities significantly lower than the initial ones. This is the process depicted in Fig. 7. Owing to the small effective mass of the soliton, any numerical uncertainty in the energy of the system is translated into a significant error in the final velocity, so the graph in Fig. 8, showing the relations between initial and final velocities, is only indicative. We cannot rule out the possibility of narrow windows, in which the solitons are trapped in bound states, as in the $\varphi^4$ theory. The energy lost during the collision is left in a breather mode, indistinguishable from the ones described in the preceding paragraph. It follows from this discussion that neutral solitons can bind; this excitation changes smoothly into a breather as the mean separation between the soliton decreases.

The SSH Hamiltonian has no obvious equivalence principle between different frames of reference. In the undimerized case, electrons behave like massless relativistic particles with velocity equal to the Fermi velocity, and the corresponding value for the phonons is the sound velocity; the same discrepancy persists in the broken-symmetry state. Hence, we have analyzed soliton-antisoliton collisions in other frames of reference to see if the description outlined above also holds. Figure 9 shows the evolution of a soliton at rest and another hittting it at its maximum velocity. It can be seen that most of the kinetic energy is transferred from one soliton to the other, as if there were some kind of equivalence principle, and the momenta of the solitons were conserved.

When the Fermi energy is raised or lowered, to simulate collisions between charged solitons, the above processes change, and the solitons no longer pass through each other, as shown in Fig. 10. We think this effect is related to

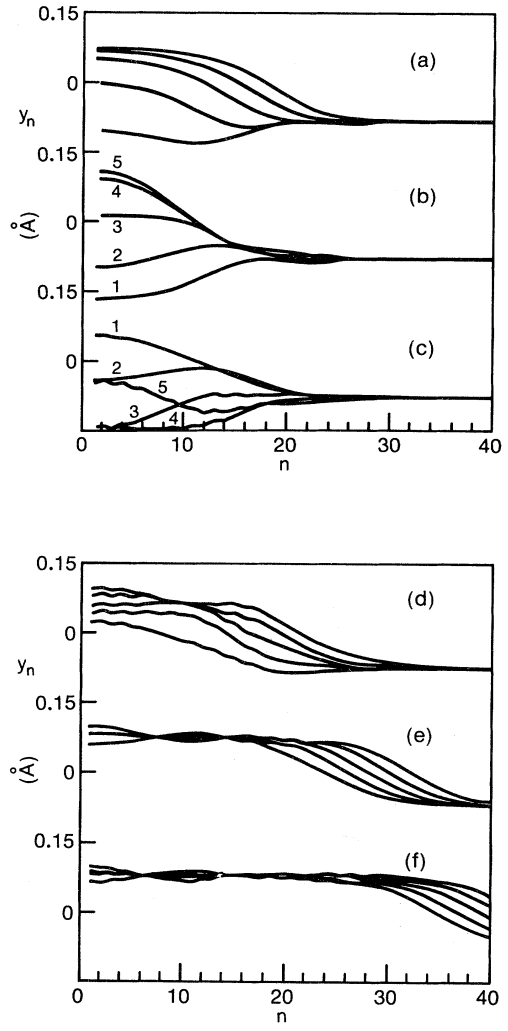


FIG. 7. As in Fig. 6. Initial velocity of the solitons is 4.8 cm/s.

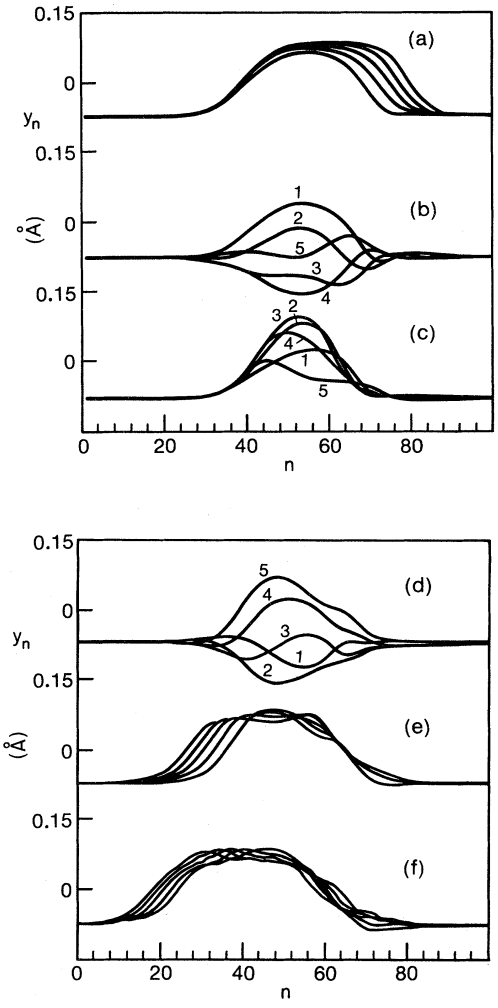


FIG. 9. Collision of a soliton initially moving at 4.7 cm/s with an antisoliton at rest in a ring of 100 atoms. Time intervals as in Figs. 6 and 7.

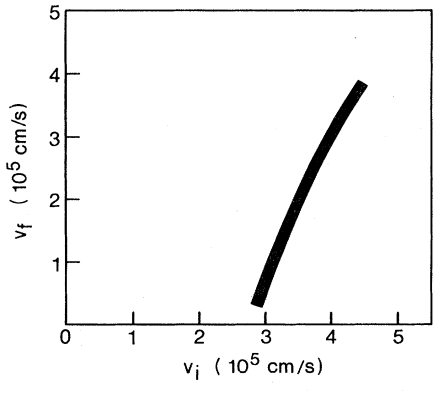


FIG. 8. Final versus initial velocity of a soliton after undergoing a collision with an antisoliton in the rest frame of reference of the pair.

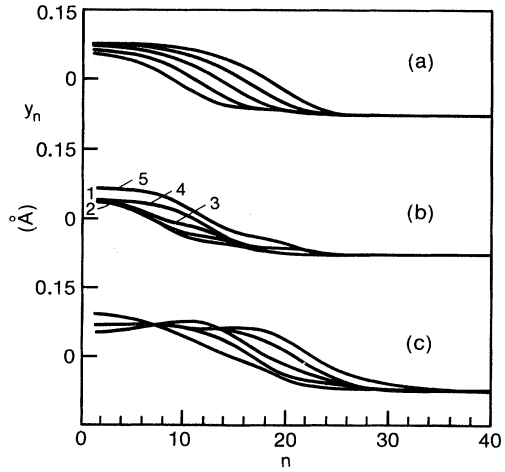


FIG. 10. Collision between charged solitons. Initial conditions as in Fig. 7 but the chemical potential of the chain has been lowered to −0.3 eV, so the midgap states are empty.

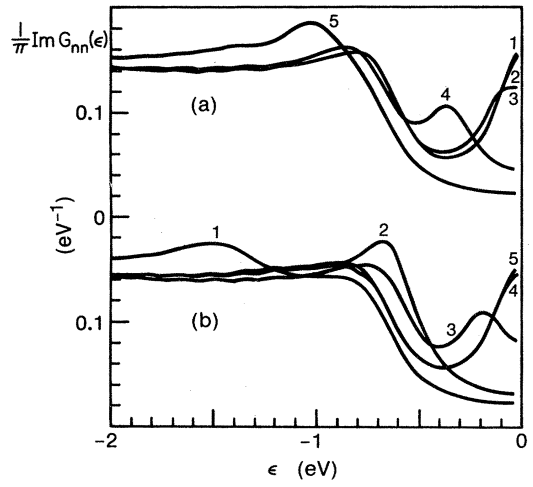


FIG. 11. Average density of states for the 60 atoms around the center of mass of a soliton-antisoliton system undergoing a collision. Only the valence band is shown. A Lorentzian widening of 0.15 eV has been included. Situations depicted in (a) and (b) correspond exactly to the ionic positions shown in Figs. 7(b) and 7(c).

the outward pressure exerted by the extra localized electrons present in the system, in a way closely related to the effect that allows the formation of polarons.[16]

Finally, it is interesting to discuss the effect of collisions on the electronic density of states. Only the region around the gap is perturbed, and the results are shown in Fig. 11. The main effect is the splitting of the midgap state, which moves into the conduction and valence bands, and is consequently broadened. At the point when the order parameter is above its normal value, the "local gap" increases slightly, as expected. Electrons or holes which are initially in the midgap state can be transferred to the conduction or valence bands of the chain during this process, and so we think soliton-antisoliton collisions can be an effective charge-transfer and neutralization mechanism for solitons.

## V. CONCLUSIONS

We have presented a detailed study of the nonlinear excitations of neutral polyacetylene chains. Solitons are very close to the predictions of the continuum model, except for a small ($\sim 0.15$ Å) shrinking of the chain around it (it is to be stressed that we are working with the standard set of interaction parameters,[2] which predict a fairly large width, $14a$, $a$ being the length of the C—C bond, for the soliton). There is a maximum velocity, $4.8\times 10^6$ cm/s, above which the soliton cannot propagate.

Another relevant excitation, the breather, has also been described. It has been shown to be built up of optical phonons with wavelength of $\sim 15a$, kept in a coherent state of about $(30\text{—}40)a$ by their nonlinear interactions. The lifetime of this mode is very large compared with typical phonon periods.

These two modes are highly stable and retain their shape after undergoing collisions among themselves. The soliton-antisoliton collision has been studied in great detail. The order parameter behaves in a similar way to what has been found in numerical analysis of the $\varphi^4$ classical field. Solitons start to pass through each other, and then move away in times comparable to the optical-phonon frequency. The details of the collision are affected by the charge state of the solitons.

For velocities below a given threshold (in the center-of-mass frame of reference) solitons are bound and cannot separate to infinity. Above it, the final velocity continuously increases as a function of the initial velocity, part of the energy being transferred to a breather mode left at the place where the collision took place. Again, the order parameter varies smoothly over regions large compared with the lattice constant, so these processes should be well described by a continuum theory.

The main effect of soliton-antisoliton collisions on the electronic properties is the splitting of the midgap states, which can be as large as 4 eV. These states become resonances in the conduction and valence bands. This effect may provide an efficient charge-transfer mechanism among solitons.

## ACKNOWLEDGMENTS

I am grateful to J. R. Schrieffer for many useful suggestions and discussions during the course of this work. This material is based upon research supported in part by the National Science Foundation under Grant No. PHY77-27084, supplemented by funds from the National Aeronautics and Space Administration.

## APPENDIX

We will examine first the case depicted in Fig. 12, that is, the calculation of the electronic structure of an infinite chain of which $n$ central atoms are displaced from their regular positions. The number of atoms and the phases at both ends are arbitrary.

It can be shown that for the perfect parts of the right-hand and to the left-hand sides of the displace portions, the quantities

$$T(\omega)=\frac{G_{i+1,j}(\omega)}{G_{i,j}(\omega)} \quad \text{(for the right-hand side)},$$
$$T'(\omega)=\frac{G_{i-1,j}(\omega)}{G_{i,j}(\omega)} \quad \text{(for the left-hand side)} \tag{A1}$$

are functions independent of $j$, which, for the particular case of dimerized polyacetylene, can be calculated analytically.[2]

Within the central part, we have to solve the following equation:

$$\omega G_{i,j}(\omega)=t_i G_{i+1j}(\omega)+t_{i-1}G_{i-1,j}(\omega)+\delta_{i,j} \tag{A2}$$

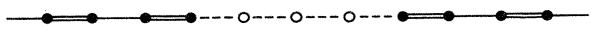

FIG. 12. Sketch of the geometries analyzed in this work. Solid circles denote clamped atoms. Open circles denote atoms which are allowed to move. See Appendix for details.

where $t_i$ is the hopping element of the Hamiltonian between orbitals located at atoms $i$ and $i+1$:

$$t_i = t + \alpha(x_{i+1} - x_i) \ . \tag{A3}$$

We define the following functions:

$$T_i(\omega) = \frac{G_{i,j}(\omega)}{G_{i-1,j}(\omega)}, \quad T_i'(\omega) = \frac{G_{i-1,j}(\omega)}{G_{i,j}(\omega)} \ , \tag{A4}$$

which now depend explicitly on the position along the chain, $i$, although independent of the second index, $j$.[8] From Eq. (A2) these functions satisfy

$$\begin{aligned} \omega T_i(\omega) &= t_i T_i(\omega) T_{i+1}(\omega) + t_{i-1} \ , \\ \omega T_i'(\omega) &= t_{i-1} + t_{i-2} T_i'(\omega) T_{i-1}'(\omega) \ , \end{aligned} \tag{A5}$$

so that

$$T_i(\omega) = \frac{t_{i-1}}{\omega - t_i T_{i+1}(\omega)}, \quad T_i'(\omega) = \frac{t_{i-1}}{\omega - t_{i-2} T_{i-1}'(\omega)} \ . \tag{A6}$$

Since we know the boundary conditions (A1) we can iterate Eqs. (A6) and obtain these functions for the entire displaced portion of the chain. In terms of these functions we can write

$$\begin{aligned} G_{i,i}(\omega) &= \frac{1}{\omega - t_{i-1} T_i'(\omega) - t_i T_{i+1}(\omega)} \ , \\ G_{i+1,i}(\omega) &= T_{i+1}(\omega) G_{i,i}(\omega) \ , \end{aligned} \tag{A7}$$

which finishes the calculation. All the information about the boundary conditions is included in the initial transfer functions (A1). In particular, by setting

$$T(\omega) = T'(\omega) = 0 \ , \tag{A8}$$

we can obtain the properties of a finite chain with open ends.

The case of a ring is slightly more complicated, and this method cannot be used in a straightforward way. To do this calculation, we begin by setting an arbitrarily chosen hopping integral $t_n = 0$. The Green's functions for this case are obtained using the method described above. In order to estimate the complete Green's functions we now have to solve the following Koster-Slater equation:[7]

$$\begin{aligned} G_{i,j}(\omega) = G_{i,j}^0(\omega) + t_n [ \, & G_{i,n}^0(\omega) G_{n+1,j}(\omega) \\ & + G_{i,n+1}^0(\omega) G_{n,j}(\omega) ] \ , \end{aligned} \tag{A9}$$

where $G_{i,j}^0(\omega)$ has been calculated previously.

The particular case of $G_{n,j}(\omega)$ and $G_{n+1,j}(\omega)$ split into sets of two coupled equations for each $j$ easily solvable:

$$\begin{aligned} G_{n,j}(\omega) &= G_{n,j}^0(\omega) + t_n [ \, G_{n,n}^0(\omega) G_{n+1,j}(\omega) \\ &\quad + G_{n,n+1}^0(\omega) G_{n,j}(\omega) ] \ , \\ G_{n+1,j}(\omega) &= G_{n+1,j}^0(\omega) + t_n [ \, G_{n+1,n}^0(\omega) G_{n+1,j}(\omega) \\ &\quad + G_{n+1,n+1}(\omega) G_{n,j}(\omega) ] \ , \end{aligned} \tag{A10}$$

which are solved. It is easy to see that, in terms of these functions, all Green's functions can be calculated using Eq. (A9).

*On leave from Departamento Física del Estado Sólido, Universidadad Autónoma, Cantoblanco, Madrid 34 Spain.

[1]W. P. Su, J. R. Schrieffer, and A. J. Heeger, Phys. Rev. Lett. **42**, 1698 (1979).
[2]W. P. Su, J. R. Schrieffer, and A. J. Heeger, Phys. Rev. B **22**, 2099 (1980).
[3]W. P. Su, and J. R. Schrieffer, Proc. Natl. Acad. Sci. U.S.A. **77**, 5626 (1980).
[4]A. R. Bishop, D. K. Campbell, P. S. Lomdahl, B. Horovitz, and S. R. Phillpot, Phys. Rev. Lett. **52**, 671 (1984).
[5]G. B. Blanchet, C. R. Fincher, T. C. Chung, and A. J. Heeger, Phys. Rev. Lett. **50**, 1938 (1983).
[6]J. E. Hirsch and E. Fradkin, Phys. Rev. Lett. **49**, 402 (1982).
[7]M. Nakahara and K. Maki, Phys. Rev. B **25**, 7789 (1982).
[8]L. Falicov and F. Yudurain, J. Phys. C **8**, 147 (1975).
[9]V. Heine, in *Solid State Physics,* edited by H. Ehrenreich, F. Seitz, and D. Turnbull (Academic, New York, 1980), Vol. 35, p. 1.
[10]S. A. Brazovskii, Zh. Eksp. Teor. Fiz. **78**, 677 (1980) [Sov. Phys.—JETP **51**, 342 (1980)].
[11]H. Takayama, Y. R. Lin Liu, and K. Maki, Phys. Rev. B **21**, 2388 (1980).
[12]S. Jedayev, Phys. Rev. B **28**, 3447 (1983).
[13]R. R. Chance, D. S. Boudreaux, J. L. Brédas, and R. Silbey, Phys. Rev. B **27**, 1440 (1983).
[14]See, for instance, A. R. Bishop, in *Physics In One Dimension,* edited by J. Bernasconi and T. Schneider (Springer, Berlin, 1981).
[15]D. K. Campbell, J. F. Schonfeld, and C. A. Wingate (unpublished).
[16]D. K. Campbell and A. R. Bishop, Nucl. Phys. **297** (1982).